Compressed quantitative acoustic microscopy

Jonghoon Kim, Paul Hill, Nishan Canagarajah, Daniel Rohrbach, Denis Kouamé, Jonathan Mamou, Alin Achim, Adrian Basarab

COMPRESSED QUANTITATIVE ACOUSTIC MICROSCOPY

J-H. Kim[1], P.R. Hill[1], N. Canagarajah[1], D. Rohrbach[2], D. Kouamé[3], J. Mamou[2], A. Achim[1⋆] and A. Basarab[3⋆]

[1]Visual Information Laboratory, University of Bristol, United Kingdom
[2]Lizzi Center for Biomedical Engineering, Riverside Research, NYC, New York, USA
[3]IRIT, UMR CNRS 5505, University of Toulouse, Université Paul Sabatier, Toulouse, France
⋆*Shared last authors*

ABSTRACT

Scanning acoustic microscopy is a well-accepted modality for forming quantitative 2D maps of acoustic properties of soft tissues at microscopic scales. In our studies, the sample is raster-scanned with a spatial step size of 2 μm using a 250 MHz transducer resulting in 3D RF data cubes. Each RF signal is processed to obtain, for each spatial location, acoustic parameters, e.g., the speed of sound. The scanning time is directly dependent on the sample size and can range from few minutes to hours. In order to maintain constant experimental conditions for the sensitive thin sectioned samples, the scanning time is an important practical issue. Hence, the main objective of this work is to reduce the scanning time by reconstructing acoustic microscopy images from spatially under sampled measurements, based on the theory of compressive sampling. A recently proposed approximate message passing method using a Cauchy maximum a posteriori image denoising algorithm is thus employed to account for the non-Gaussianity of quantitative acoustic microscopy wavelet coefficients.

Index Terms— scanning acoustic microscopy, compressive sampling, approximate message passing, Cauchy distribution

I. INTRODUCTION

Quantitative acoustic microscopy (QAM) is an imaging technology employed to investigate soft biological tissue at microscopic resolution by eliciting its mechanical property with very high frequency ultrasound [1]. Specifically, by processing RF echo data, QAM yields two-dimensional (2D) quantitative maps of the acoustical and mechanical properties of soft tissues. Therefore, QAM provides a novel contrast mechanism compared to histology photomicrographs and optical and electron microscopy images [2]. Currently, QAM requires a complete 2D raster scan of the sample to form images, thus yielding a large amount of RF data and leading to corresponding acquisition time when using a conventional spatial sampling scheme. In this study, the data acquisition corresponds to a 2 μm step raster scan at 250 MHz.

The scanning time is directly dependent on the sample size and can range from few minutes to hours. In order to maintain constant experimental conditions for the sensitive thin sectioned samples, the scanning time is an important practical issue. Hence, the main objective of this work is to reduce the scanning time by reconstructing QAM images from spatially under sampled measurements, based on the theory of compressive sampling (CS). In this work, an approximate message passing (AMP) algorithm, previously shown to outperform l_1-norm minimization, was implemented. This study demonstrates that a discrete wavelet transform is an appropriate choice for SAM. The Cauchy distribution was used to construct the denoising function embedded in the proposed AMP algorithm [3].

The contribution of the proposed AMP-based QAM imaging framework is twofold: (i) to propose a spiral spatial sampling scheme that meets the practical constraints of QAM acquisition, (ii) to design a dedicated wavelet domain AMP-based reconstruction algorithm, which exploits underlying data statistics through the use of a Cauchy-based MAP algorithm.

The remainder of this paper is organized as follows. Section II provides a brief background on QAM, CS and AMP. Section III introduces the spiral sampling and the AMP-based reconstruction algorithm. Section IV compares the performance of the proposed method with a standard AMP algorithm. Finally, conclusions are reported in Section V.

II. BACKGROUND

II-A. Quantitative Acoustic Microscopy

In QAM, a high-frequency (e.g., > 50 MHz), single-element, spherically-focused (e.g., F-number < 1.3), transducer transmits a short ultrasound pulse and receives the RF echo signals reflected from the sample which consists of a thin section of soft tissue affixed to a microscopy slide. At each scan location, the RF data is digitized, saved, and

Part of this work has been supported by the thematic trimester on image processing of the CIMI Labex, Toulouse, France, under grant ANR-11-LABX-0040-CIMI within the program ANR-11-IDEX-0002-02 and by ProSmart Solutions, 6-12 Rue Andras Beck 92360 Meudon, France.

processed offline to yield values of acoustic parameters such as the speed of sound used in this study [4]. The values obtained at each scan location are then combined to form quantitative 2D parameter maps.

II-B. Compressive Sensing

CS theory guarantees an exact recovery of specific signals or images from fewer measurements than the number predicted by the Nyquist limit [5], [6]. This guarantee is mainly based on two conditions: the images must have a sparse representation in a given basis or frame and the measurement and sparsity bases should be as much decorrelated as possible (*i.e.*, incoherent measurements). In contrast to the classical sampling followed by compression procedure, CS is concerned with sampling signals more parsimoniously, acquiring only the relevant signal information. CS measurement model is

$$\mathbf{y} = \mathbf{\Phi x} + \mathbf{n}, \tag{1}$$

where $\mathbf{y} \in \mathbb{R}^M$ is the measurement vector, $\mathbf{x} \in \mathbb{R}^N$ is the image to be reconstructed ($N >> M$), $\mathbf{\Phi} \in \mathbb{R}^{M \times N}$ is the measurement matrix and $\mathbf{n} \in \mathbb{R}^M$ is an additive white Gaussian noise.

Recovering the fully-sampled image $\mathbf{x}$ from the measurements $\mathbf{y}$ have received a considerable attention in the literature. Among the existing reconstruction methods, we focus in this study on AMP algorithm, an iterative process performing sparse representation-based image denoising, because of its low computational cost and fast convergence performance [7], [8].

II-C. Approximate Message Passing Reconstruction

In the context of CS, AMP reconstructs an original image from a reduced number of linear measurements by performing elementwise denoising at each iteration. Reconstructing the image amounts to successive noise cancellations until the noise variance decreases to a satisfactory level. The algorithm can be succinctly summarised through the following two steps:

$$\mathbf{x}^{t+1} = \eta_t \left(\mathbf{\Phi}^T \mathbf{z^t} + \mathbf{x^t} \right), \tag{2}$$

$$\mathbf{z^t} = \mathbf{y} - \mathbf{\Phi x^t} + \frac{1}{\delta} \mathbf{z^{t-1}} \langle \eta'_{t-1} \left(\mathbf{\Phi}^T \mathbf{z^{t-1}} + \mathbf{x^{t-1}} \right) \rangle, \tag{3}$$

where $\mathbf{x}, \mathbf{y}, \mathbf{z}$ and δ denote a sparse image (in lexicographical order), the measurements, the residual and the undersampling ratio (M/N) respectively. $\eta(\cdot)$ is a function that represents the denoiser, $\eta'(\cdot)$ is its first derivative and $\langle \mathbf{x} \rangle = \frac{1}{N} \sum_{i=1}^{N} (x_i)$. The superscript t represents the iteration number and $(\cdot)^T$ stands for the classical conjugate transpose. Given $\mathbf{x} = \mathbf{0}$ and $\mathbf{z} = \mathbf{y}$ as an initial condition, the algorithm iterates sequentially (2) and (3) until satisfying a stopping criterion or reaching a pre-set iteration number. The last term of the right hand side in (3) is referred to as the Onsager reaction term and serves at balancing the sparsity-undersampling tradeoff [9], [10].

An extended wavelet-based AMP system can be generated by integrating a wavelet transform (denoted by W) into (2) and (3) using the following transformation.

$$\mathbf{y} = \mathbf{\Phi} \underbrace{W^{-1} \boldsymbol{\theta}_{\mathbf{x}}}_{\mathbf{x}} + \mathbf{n}, \tag{4}$$

where W^{-1} is the inverse wavelet transform, W and $\theta_{\mathbf{x}}$ denotes the sparse representation of $\mathbf{x}$ within wavelet domain. Denoting $\mathbf{\Phi} W^{-1}$ by $\mathbf{\Theta}$, (2) and (3) turn into:

$$\theta_{\mathbf{x}}^{\mathbf{t+1}} = \eta_t \left(\mathbf{\Theta^T z^t} + \theta_{\mathbf{x}}^{\mathbf{t}} \right), \tag{5}$$

$$\mathbf{z^t} = \mathbf{y} - \mathbf{\Theta} \theta_{\mathbf{x}}^{\mathbf{t}} + \frac{1}{\delta} \mathbf{z^{t-1}} \left\langle \eta'_{t-1} \left(\mathbf{\Theta^T z^{t-1}} + \theta_{\mathbf{x}}^{\mathbf{t-1}} \right) \right\rangle. \tag{6}$$

The subsequently defined denoising algorithms seek to denoise the elements of $\theta_{\mathbf{q}}^{\mathbf{t}} = \mathbf{\Theta^T z^t} + \theta_{\mathbf{x}}^{\mathbf{t}}$ corresponding to the contaminated wavelet coefficients. To simplify the following notation, the ith element of $\theta_{\mathbf{q}}^{\mathbf{t}}$ is defined as $\theta_{\mathbf{q},i}^{t} = v$ and the ith element of the denoised output $\theta_{\mathbf{x}}^{\mathbf{t+1}}$ is defined as $\theta_{\mathbf{x},i}^{t+1} = \hat{w}$ (a denoised estimate of the true coefficient w).

The most important design consideration is arguably the choice of the shrinkage (denoising) function, η, in (5) above. Assuming that the clean wavelet coefficients can be statistically modelled by Laplace distribution, soft threshold denoiser is a classical choice for η [9]. Therefore, we use it herein as a comparative method .

Soft Threshold (ST) denoiser:

$$\begin{aligned} \hat{w} = \eta(v) &= \text{sign}(v)(|v| - \tau) \cdot \mathbb{1}_{(|v|>\tau)}, \\ \eta'(v) &= \mathbb{1}_{(|v|>\tau)}, \end{aligned} \tag{7}$$

where $\mathbb{1}_{(\cdot)}$ is the indicator function. The threshold τ is defined as the M^{th} largest magnitude value of $\theta_{\mathbf{q}}^{\mathbf{t}}$ [9].

III. COMPRESSED QAM IMAGING

III-A. Sensing pattern

The incoherence between the sensing matrix and the sparsifying transform is important in CS applications. Therefore, theoretically optimal sensing matrices are based on randomness. For instance, image projections on random Gaussian vectors or point-wise multiplication with Bernoulli vectors formed by uniformly random distributed zeros and ones are classical examples of obtaining measurements with maximum incoherence with respect to deterministic sparsifying transforms. However, they are impractical for QAM data acquisition given that RF data are typically acquired

continuously as the motor stages are moved.
In order to respect the acquisition constraints, this paper investigates a spiral pattern shown in Fig. 1, which can be easily implemented using servo motors.

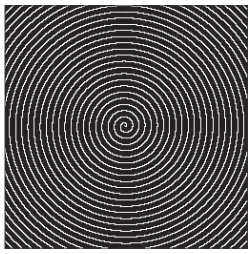

Fig. 1: Proposed spiral pattern for sample scanning in QAM.

III-B. Cauchy-based denoiser

This section provides the derivation of the Cauchy-based denoiser in the wavelet domain embedded in the proposed AMP algorithm. Wavelet coefficients can be accurately modelled using heavy tailed distributions such as the $\alpha-$stable distribution [11], [12]. The Cauchy distribution is a special case of the $\alpha-$stable family which not only has a heavy tailed form but has a compact analytical probability density function given by [13]:

$$P(w) = \frac{\gamma}{w^2 + \gamma^2}, \tag{8}$$

where w and γ are the wavelet coefficient value and the dispersion parameter respectively. Given (8), a maximum *a posteriori* (MAP) estimator method (9) can lead to the derivation of explicit formulae (12) estimating a clean wavelet coefficient w from an observed coefficient observation v contaminated with additive Gaussian noise (i.e. $n = v - w$ and noise variance σ^2) [14].

$$\hat{w} = arg\max_{w} P_{w|v}(w|v). \tag{9}$$

Assuming an additive Gaussian noise, *i.e.* $P_{v|w}(v|w) \sim N(0, \sigma^2)$, and using Bayes' rule, the MAP estimator is given in (10). Note that (10) is obtained using the log-posterior and ignoring the evidence $P_v(v)$ which is constant for all inputs.

$$\hat{w}(v) = arg\max_{w}\left[-\frac{(v-w)^2}{2\sigma^2} + log\left(\frac{\gamma}{w^2+\gamma^2}\right)\right]. \tag{10}$$

To find the solution to (10), we cancel the first derivative relative to w of the function in (10):

$$\hat{w}^3 - v\hat{w}^2 + (\gamma^2 + 2\sigma^2)\hat{w} - \gamma^2 v = 0. \tag{11}$$

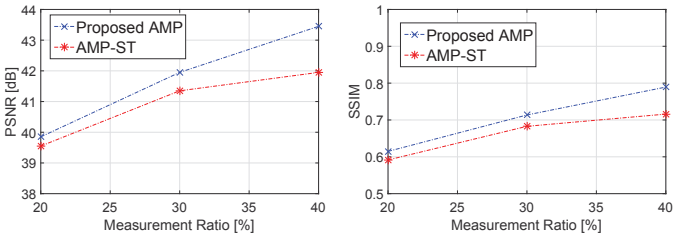

(a) (b)

Fig. 2: Evolution of PSNR and SSIM for different measurement ratios for the proposed AMP and existing AMP-ST algorithms.

Using Cardano′s method, the estimate of w can be found in (12) of which first derivative is (13).

$$\hat{w} = \eta(v) = \frac{v}{3} + s + t, \tag{12}$$

$$\hat{w}^{'} = \eta^{'}(v) = 1/3 + s^{'} + t^{'}, \tag{13}$$

where s and t are values determined by v and σ^2 iteratively updated at each iteration together with a constant value γ; σ^2 is estimated as the variance of the $\mathbf{z}$ vector defined in (3). s and t are defined as:

$$\begin{gathered} s = \sqrt[3]{\frac{q}{2} + dd}, \quad t = \sqrt[3]{\frac{q}{2} - dd}, \\ dd = \sqrt{p^3/27 + q^2/4}, \\ p = \gamma^2 + 2\sigma^2 - v^2/3, \\ q = v\gamma^2 + 2v^3/27 - (\gamma^2 + 2\sigma^2)v/3. \end{gathered} \tag{14}$$

s' and t' are found as follows:

$$\begin{gathered} s' = \frac{q'/2+dd'}{3(q/2+dd)^{(2/3)}}, \quad t' = \frac{q'/2-dd'}{3(q/2-dd)^{(2/3)}}, \\ dd' = \frac{p'p^2/9+q'q/2}{2dd}, \\ p' = -2v/3, \\ q' = -2\sigma^2/3 + 2\gamma^2/3 + 2v^2/9. \end{gathered} \tag{15}$$

IV. RESULTS

The proposed method was validated on QAM data classically acquired at 250 MHz from a human lymph node thin section obtained from a colorectal cancer patient. The fully sampled image corresponds to standard raster scanning at conventional spatial scanning frequencies, resulting into a pixel size of 2 μm per 2 μm. The data was further downsampled using the spiral pattern in Fig. 1 in order to generate the compressed measurements. Two AMP algorithms have been used to reconstruct the fully-sampled image from the spiral measurements. Both algorithms were applied in the wavelet domain, but used different denoising functions: the Cauchy denoiser proposed in Section III-B and the classical soft thresholding described in Section II-C. In the following, the two algorithms are denoted as "proposed AMP" and "AMP-ST".

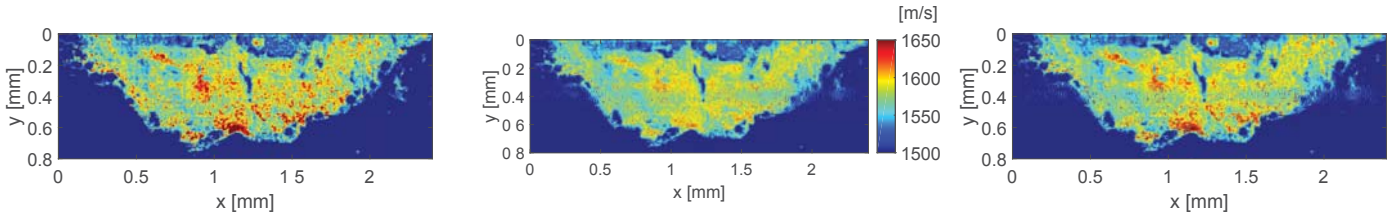

(a) (b) (c)

Fig. 3: Illustrative result showing speed-of-sound images of a thin section of a human lymph node acquired from a colorectal patient: (a) fully-sampled raster-scanned data, (b) and (c) reconstructed images from spiral sub-sampled data (measurement ratio of 30%) using the AMP-ST and proposed AMP algorithms.

In addition to visual inspection, the peak signal to noise ratio (PSNR) and the structural similarity (SSIM) index [15] were used to assess the quality of the reconstructed images by comparing them to the corresponding fully-sampled quantitative map.

Experiments were performed for measurement ratios ranging from 20% to 40% of the data obtained using the conventional raster scanning approach. Fig. 2 displays the resulting PSNR and SSIM values. The quantitative results indicate that the proposed AMP always provided higher PSNR and SSIM than AMP-ST across the whole gamut of the investigated measurement ratios. Three speed-of-sound maps are shown in Fig. 3 representing the fully-sampled image, and the ones recovered by AMP-ST and proposed AMP algorithms from data generated with the spiral pattern for a measurement rate of 30%. From the visual perception, it can be seen that the dense red area is better reconstructed using the proposed AMP than with AMP-ST. This subjective assessment is consistent with the quantitative results shown in Fig. 2.

Note that similar results can be obtained for other acoustic parameter maps including attenuation or impedance [3].

V. CONCLUSIONS

Speed-of-sound maps of cancerous human lymph nodes were reconstructed using an AMP algorithm embedding a Cauchy-based denoising function from compressed spiral data. The reconstruction results were more accurate than the ones obtained using the existing AMP algorithm coupled with the soft thresholding denoiser. In addition to the sample reduction, the spiral pattern allows fast scanning because it is an indefinitely differentiable continuous curve easily implementable with servo motors. For a measurement ratio of 30%, the proposed spiral scanning pattern is expected to reduce the scan time by 60%.

REFERENCES

[1] M. F. Marmor, H. K. Wickramasinghe, and R. A.Lemons, "Acoustic microscopy of the human retina and pigment epithelium," Invest. Ophthalmol. Vis. Sci., vol. 16, no. 7, pp. 660-666, Jul. 1977.

[2] J. A. Hildebrand, D. Rugar, R. N. Johnston and C. F. Quate, "Acoustic microscopy of living cells," Proc. Nat. Academy. Sci., USA Vol. 78, no. 3, pp.1656-1660, Mar. 1981.

[3] J-H. Kim, J. Mamou, P.R. Hill, N.Canagarajah, D. Kouamé, A. Basarab and A. Achim1, "Approximate Message Passing Reconstruction of Quantitative Acoustic Microscopy Images," in press, 2017.

[4] D. Rohrbach, A. Jakob, H. Lloyd, S. Tretbar, R. Silverman, and J. Mamou, "A Novel Quantitative 500-MHz Acoustic-microscopy System for Ophthalmologic Tissues," IEEE Transactions on Biomedical Engineering, pp.715 - 724, May. 2016.

[5] E. Candes, J. Romberg, and T. Tao, "Robust uncertainty principles: exact signal reconstruction from highly incomplete frequency information," Information Theory, IEEE Transactions on, vol. 52, pp. 489-509, Feb. 2006.

[6] D. Donoho, "Compressed sensing," Information Theory, IEEE Transactions on, vol. 52, pp. 1289-1306, Apr. 2006.

[7] T. Blumensath and M. Davies, "Iterative hard thresholding for compressed sensing," Applied and Computational Harmonic Analysis, vol. 27, no. 3, pp. 265-274, 2009.

[8] D. Donoho, "De-noising by soft-thresholding," Information Theory, IEEE Transactions on, vol. 41, no. 3, pp. 613-627, 2002.

[9] D. L. Donoho, A. Maleki, and A. Montanari, "Message passing algorithms for compressed sensing," Proc. Nat. Academy Sci., vol. 106, no. 45, pp. 18914-18919, Nov. 2009.

[10] C.A. Metzler, A. Maleki and R.G. Baraniuk, "From denoising to compressed sensing," arXiv preprint arXiv:1406.4175, 2014.

[11] A. Achim, A. Bezerianos, and P. Tsakalides, "Novel Bayesian multiscale method for speckle removal in medical ultrasound images," IEEE Transactions on Medical Imaging, 20(8), pp. 772-783, 2001.

[12] A. Achim and E. E. Kuruoglu, "Image denoising using bivariate α-stable distributions in the complex wavelet domain," in IEEE Signal Processing Letters, vol. 12, no. 1, pp. 17-20, Jan. 2005.

[13] P. R. Hill, J. H. Kim, A. Basarab, D. Kouamé, D. R. Bull and A. Achim, "Compressive imaging using approximate message passing and a Cauchy prior in the wavelet domain," 2016 IEEE International Conference on Image Processing (ICIP), Phoenix, AZ, USA, 2016, pp. 2514-2518.

[14] J. Ilow and D. Hatzinakos, "Analytic alpha-stable noise modeling in a Poisson field of interferers or scatterers," IEEE Transactions on Signal Processing, vol. 46, pp. 1601-1611, Jun. 1998.

[15] Z. Wang, A. C. Bovik, H. R. Sheikh and E. P. Simoncelli, "Image quality assessment: from error visibility to structural similarity," IEEE Transaction on Image Processing, vol. 13, no. 4, pp. 600-612, Apr. 2004.